Enhanced Dual Visible Light Fluorescence from the 2,2′-Dipyridyl Tungsten Alkylidyne Complex [W(≡$CC_6H_4NMe_2$-4)(O_2CCF_3)$(CO)_2${κ²-2,2′-$(NC_5H_4)_2$}]: An Organometallic Twisted Intramolecular Charge Transfer State

Paul A. Jelliss* and Keith M. Wampler

Department of Chemistry, Saint Louis University, St. Louis, Missouri 63103

Aleksander Siemiarczuk

Fast Kinetics Application Laboratory, Photon Technology International (Canada) Inc., 347 Consortium Court, London, Ontario, Canada N6E 2S

Received September 8, 2004

The *N*,*N*-dimethylanilino tungsten alkylidyne complex [W(≡$CC_6H_4NMe_2$-4)(O_2CCF_3)$(CO)_2$-$(NC_5H_4Me\text{-}4)_2$] has been synthesized, characterized, and employed as a precursor to neutral and cationic 2,2′-dipyridyl and TMEDA (*N*,*N*,*N*′,*N*′-tetramethylethylenediamine) complexes, which display dual blue and yellow fluorescences in CH_2Cl_2 solutions at ambient temperatures with surprisingly high quantum yields for this class of organometallic complex. The efficiencies of the radiative emissions from the 2,2′-dipyridyl complex [W(≡$CC_6H_4NMe_2$-4)(O_2CCF_3)$(CO)_2${κ²-2,2′-$(NC_5H_4)_2$}] are particularly impressive. The dual nature of the emissions ($\lambda_{em} \approx$ 450 and 540−580 nm) is attributed to independent, short-lived (ns) "twisted intramolecular charge transfer" (^{1}TICT) and $^1d_W-\pi^*_{W\equiv CAr}$ states, respectively, the former being well understood in organic aromatic systems, but yet to be described for organometallic complexes.

Introduction

The emission of visible light from polypyridyl tungsten(0) d^6 complexes is well established,[1] while the photophysics of group 6 metal Fischer alkylidyne complexes, though somewhat less studied,[2] is nevertheless of topical relevance to the quest for the development of light-emitting metal complexes for applications in molecular electronic control, communication, and sensing.[3] Photoluminescence from low-valent organometallic species is unusual, given the propensity for such complexes to undergo ligand dissociation as the primary photoprocess,[4] or in the case of Fischer alkylidynes, to be activated to further reactivity resulting in ligand-based transformations or metal-centered radical reactions.[3e,5,6] Photoluminescence from metal alkylidyne complexes has been specifically reviewed by Hopkins.[7] Low quantum yield emission of red light ($\lambda_{em} \approx$ 750 nm, $\Phi_{em} \leq 6.9 \times 10^{-4}$) has been observed with the complexes [M(≡CAr)(CO){$P(OMe)_3$}(η^5-C_5H_5)] (**1**, M = W, Mo; Ar = Ph, C_6H_4Me-2, $C_{10}H_7$-2) and attributed to a $^3d_M-\pi^*_{M\equiv CAr}$ triplet state.[8] Of particular note are the complexes [W(≡CR)Cl$(CO)_2$(κ²-L_2)] (**2a**, R = Ph, L_2 = TMEDA; **2b**, R = Bu^t, L_2 = TMEDA; **2c**, R = Ph, L_2 = 2,2′-dipyridyl) (Chart 1).[9] Mayr et al. have observed orange emission (λ_{em} = 640 nm) from complex **2a**,

* To whom correspondence should be addressed. E-mail: jellissp@slu.edu.

(1) (a) Lees, A. J. *Coord. Chem. Rev.* **1998**, *177*, 3. (b) Stufkens, D. J. *Coord. Chem. Rev.* **1990**, *104*, 39. (c) Rawlins, K. A.; Lees, A. J. *Inorg. Chem.* **1989**, *28*, 2154. (d) Manuta, D. M.; Lees, A. J. *Inorg. Chem.* **1986**, *25*, 1354. (e) Manuta, D. M.; Lees, A. J. *Inorg. Chem.* **1986**, *25*, 3212. (f) Servaas, P. C.; van Dijk, H. K.; Snoeck, T. L.; Stufkens, D. J.; Oskam, A. *Inorg. Chem.* **1985**, *24*, 4494. (g) Manuta, D. M.; Lees, A. J. *Inorg. Chem.* **1983**, *22*, 3825. (h) Balk, R. W.; Stufkens, D. J.; Oskam, A. *Inorg. Chem.* **1980**, *19*, 3015. (i) Balk, R. W.; Stufkens, D. J.; Oskam, A. *Inorg. Chim. Acta* **1978**, *28*, 133. (j) Wrighton, M. S.; Morse, D. L. *J. Organomet. Chem.* **1975**, *97*, 405.

(2) (a) Trammell, S.; Sullivan, B. P.; Hodges, L. M.; Harmon, W. D.; Smith, S. R.; Thorp, H. H. *Inorg. Chem.* **1995**, *34*, 2791. (b) Carter, J. D.; Kingsbury, K. B.; Wilde, A.; Schoch, T. K.; Leep, C. J.; Pham, E. K.; McElwee-White, L. *J. Am. Chem. Soc.* **1991**, *113*, 2947.

(3) (a) Long, N. J.; Kershaw, S. V. In *Optoelectronic Properties of Inorganic Compounds*; Roundhill, D. M., Fackler, J. P., Jr., Eds.; Plenum Press: New York, 1999; pp 107−159, 349−403. (b) Yam, V. W.-W.; Kam-Wing Lo, K.; Man-Chung Wong, K. *J. Organomet. Chem.* **1999**, *578*, 3. (c) McElwee-White, L.; Kingsbury. K. B.; Carter, J. D. In *Photosensitive Metal-Organic Systems. Mechanistic Principles and Applications*; Kutal, C., Serpone, N., Eds.; Advances in Chemistry 238; American Chemical Society: Washington, DC, 1993; pp 335−349.

(4) Geoffroy, G. L.; Wrighton, M. S. *Organometallic Photochemistry*; Academic Press: New York, 1976.

(5) (a) Beevor, R. G.; Freeman, M. J.; Green, M.; Morton, C. E.; Orpen, A. G. *J. Chem. Soc., Dalton Trans.* **1991**, 3021. (b) Sheridan, J. B.; Pourreau, D. B.; Geoffroy, G. L.; Rheingold, A. L. *Organometallics* **1988**, *7*, 289. (c) Mayr, A.; Asaro, M. F.; Glines, T. J. *J. Am. Chem. Soc.* **1987**, *109*, 2215. (d) Green, M. *J. Organomet. Chem.* **1986**, *300*, 93.

(6) (a) Schoch, T. K.; Orth, S. D.; Zerner, M. C.; Jørgensen, K. A.; McElwee-White, L. *J. Am. Chem. Soc.* **1995**, *117*, 6475. (b) McElwee-White, L.; Kingsbury. K. B.; Carter, J. D. *J. Photochem. Photobiol. A: Chem.* **1994**, *80*, 265. (c) Mortimer, M. D.; Carter, J. D.; McElwee-White, L. *Organometallics* **1993**, *12*, 4493. (d) Kingsbury, K. B.; Carter, J. D.; Wilde, A.; Park, H.; Takusagawa, F.; McElwee-White, L. *J. Am. Chem. Soc.* **1993**, *115*, 10056. (e) Carter, J. D.; Schoch, T. K.; McElwee-White, L. *Organometallics* **1992**, *11*, 3571.

(7) Da Re, R. E.; Hopkins, M. D. *Coord. Chem. Rev.* **2005**, submitted.

(8) Schoch, T. K.; Main, A. D.; Burton, R. D.; Lucia, L. A.; Robinson, E. A.; Schanze, K. S.; McElwee-White, L. *Inorg. Chem.* **1996**, *35*, 7769.

(9) Bocarsly, A. B.; Cameron, R. E.; Rubin, H. D.; McDermott, G. A.; Wolff, C. R.; Mayr, A. *Inorg. Chem.* **1985**, *24*, 3976.

10.1021/om0493006 CCC: $30.25
Publication on Web 01/19/2005

Chart 1

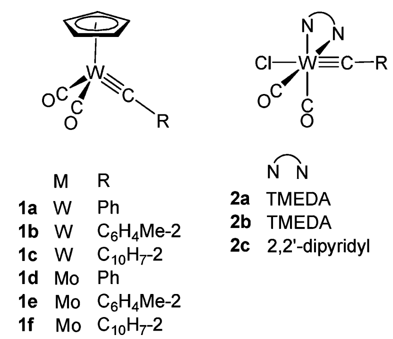

Chart 2

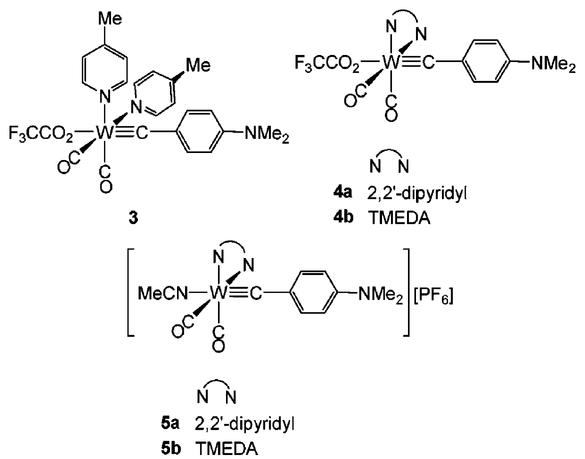

providing that the aromatic phenyl and aliphatic TMEDA are both present. The complexes became nonemissive if the aromatic group was substituted for Bu^t, as in **2b**, or the TMEDA for 2,2′-dipyridyl as in **2c**. The latter was attributed to internal quenching of $^3d_M-\pi^*_{M\equiv CPh}$ emission by the 2,2′-dipyridyl ligand. This would seem to suggest that such polypyridyl−alkylidyne ligand combinations do not represent a logical avenue of pursuit, but we report herein enhanced dual blue-yellow emission of light from just such a complex molecule and single blue emission from its derivative cationic MeCN adduct. The blue fluorescence, attributed to a twisted intramolecular charge transfer (TICT) state, is the first such photophysical response to be reported for an organometallic complex.

Results and Discussion

Synthesis and Characterization. The complex $[W(\equiv CC_6H_4NMe_2\text{-}4)(O_2CCF_3)(CO)_2(NC_5H_4Me\text{-}4)_2]$ (**3**) (Chart 2) has been synthesized by the method of Mayr,[9,10] isolated following column chromatography and fully characterized by IR spectroscopy, microanalysis (Table 1), and NMR spectroscopy (Table 2). Of particular note in this complex is the presence of the strongly electron donating NMe_2 group, the methyl groups of which were readily identified in ^1H and $^{13}C\{^1H\}$ NMR spectra at δ 3.00 (^1H) and 40.3 (^{13}C). Also identified by their diagnostic[9−11] singlet resonances at δ 277.0 and 221.4 in the $^{13}C\{^1H\}$ NMR spectrum were the alkylidyne, W≡C, and carbonyl, WCO carbons, respectively, also attesting to a C_s structure, at least in solution. The ν_{max}(CO) resonances (1976, 1886 cm^{-1}) compare well with those of the related complex $[W(\equiv CC_6H_4NH_2\text{-}4)Cl(CO)_2(NC_5H_4Me\text{-}4)_2]$ (1979, 1890 cm^{-1}), which possesses a *para*-donor amino group, NH_2, on the alkylidyne.[12] Substitution of the 4-methylpyridine ligands by a chelating 2,2′-dipyridyl in CH_2Cl_2 resulted in the quantitative formation of the complex $[W(\equiv CC_6H_4NMe_2\text{-}4)(O_2CCF_3)(CO)_2\{\kappa^2\text{-}2,2'\text{-}(NC_5H_4)_2\}]$ (**4a**) (Tables 1 and 2). Standard spectroscopic methods have been used to characterize complex **4a**. The IR spectrum is comparable with that of complex **2c** with ν_{max}(CO) resonances at 1973 and 1888 cm^{-1} (**4a**) versus 1986 and 1899 cm^{-1} (**2c**) and relatively unchanged with respect to the precursor complex **3**. These resonances appear to be relatively solvent independent, with no indication of any chemical transformation in a more polar coordinating solvent such as MeCN. From ^1H and $^{13}C\{^1H\}$ NMR spectra, the NMe_2 (δ 2.84 (^1H) and 40.3 (^{13}C)), W≡C (δ 281.3), and WCO (δ 225.0) resonances are barely adjusted with respect to the precursor **3**. Both complexes **3** and **4a** were isolated and studied as the trifluoracetato complexes rather than the more ubiquitous halo complexes, because of their greatly improved tractability on the open benchtop. Unlike the halo complexes, the trifluoroacetato complexes, which are thermodynamically stable, are not hygroscopic, rendering handling of the solid in air much easier. The complex $[W(\equiv CC_6H_4NMe_2\text{-}4)(NCMe)(CO)_2\{\kappa^2\text{-}2,2'\text{-}(NC_5H_4)_2\}][PF_6]$ (**5a**) has been synthesized in good yield by displacement of the $CF_3CO_2^-$ ligand by MeCN in the presence of $TlPF_6$. The ν_{max}(CN) resonance due to the coordinated MeCN molecule was readily identified at 2254 cm^{-1} in the IR spectrum, while the ν_{max}(CO) peaks were, as expected, shifted to higher energy (1981 and 1900 cm^{-1}) versus those of the parent neutral complex **4a**. The absence of ν_{max}(CO) resonances due to the $CF_3CO_2^-$ ligand confirmed its complete displacement. The MeCN resonances were also identified in the ^1H and $^{13}C\{^1H\}$ NMR spectra (δ 2.11 (^1H) and 1.5, 114.3 (^{13}C)), while the NMe_2 resonances were relatively unaffected by the change in charge of the complex (δ 2.91 (^1H) and 40.2 (^{13}C)).

To provide an aliphatic comparison to the 2,2′-dipyridyl complex **4a**, complex **3** was treated with *N*,*N*,*N*′,*N*′-tetramethylethylenediamine (TMEDA) to yield $[W(\equiv CC_6H_4NMe_2\text{-}4)(O_2CCF_3)(CO)_2\{\kappa^2\text{-}Me_2N(CH_2)_2NMe_2\}]$ (**4b**), by analogy with the formation of the Mayr complex **2a**. The ν_{max}(CO) resonances (1974, 1882 cm^{-1}) are close in value to both complexes **3** and **4a**, while ^1H and $^{13}C\{^1H\}$ NMR data clearly indicate the displacement of the 4-methylpyridine molecules by the chelating TMEDA ligand with resonances for the diastereotopic NMe groups at δ 2.87 and 3.16 (^1H) and at δ 58.4 and 61.5 (^{13}C). The alkylidyne aryl system is again virtually unchanged from the parent complex **3** with the alkylidyne carbon resonating at δ 279.1 and the equiva-

(10) (a) McDermott, G. A.; Dorries, A. M.; Mayr, A. *Organometallics* **1987**, *6*, 925. (b) Mayr, A.; McDermott, G. A.; Dorries, A. M. *Organometallics* **1985**, *4*, 608. (c) Hart, I. J.; Hill, A. F.; Stone, F. G. A. *J. Chem. Soc., Dalton Trans*. **1989**, 2261. (d) Dossett, S. J.; Hill, A. F.; Jeffery, J. C.; Marken, F.; Sherwood, P.; Stone, F. G. A. *J. Chem. Soc., Dalton Trans.* **1988**, 2453.

(11) (a) Hoffmeister, H.; Mayr, A. *Adv. Organomet. Chem.* **1991**, *32*, 227. (b) Gallop, M. A.; Roper, W. R. *Adv. Organomet. Chem*. **1986**, *25*, 121.

(12) Yu, M. P. Y.; Mayr, A.; Cheung, K.-K. *J. Chem. Soc., Dalton Trans*. **1998**, 475.

Table 1. Analytical and Physical Data

compound	color	yield/%	$\nu_{max}(CO)^a$/cm^{-1}	analysis^b/% C	H	N
[W(≡$CC_6H_4NMe_2$-4)(O_2CCF_3)$(CO)_2$-(NC_5H_4Me-4)$_2$], **3**	yellow	34	1976vs,^{c} 1886vs,^{c} 1688vs,^{d} 1596vs^d	44.8 (44.7)	4.1 (3.6)	6.5 (6.3)
[W(≡$CC_6H_4NMe_2$-4)(O_2CCF_3)$(CO)_2${κ^2-2,2′-$(NC_5H_4)_2$}], **4a**^{e}	red	98	1973vs,^{c} 1888vs,^{c} 1689vs,^{d} 1595vs^d	43.6 (43.1)	3.0 (2.8)	6.2 (6.6)
[W(≡$CC_6H_4NMe_2$-4)(O_2CCF_3)$(CO)_2${κ^2-$Me_2N(CH_2)_2NMe_2$}], **4b**	yellow	97	1974vs,^{c} 1882vs,^{c} 1711vs,^{d} 1605vs^d	37.5 (37.9)	4.8 (4.4)	6.8 (7.0)
[W(≡$CC_6H_4NMe_2$-4)(NCMe)$(CO)_2${κ^2-2,2′-$(NC_5H_4)_2$}][PF_6], **5a**	red	96	1981vs,^{c} 1900vs^{c,f}	39.0 (38.7)	2.9 (3.0)	7.2 (7.8)
[W(≡$CC_6H_4NMe_2$-4)(NCMe)$(CO)_2${κ^2-$Me_2N(CH_2)_2NMe_2$}][PF_6], **5b**	yellow	97	1984vs,^{c} 1892vs^{c,g}	34.0 (33.8)	4.9 (4.3)	8.6 (8.3)

^{a} Measured in CH_2Cl_2 at 298 K. ^{b} Calculated values are given in parentheses. ^{c} CO ligand. ^{d} $CF_3CO_2^-$ ligand. ^{e} Full IR spectrum (THF, 1300−2000 cm^{-1}) given in Supporting Information. ^{f} ν_{max}(CN) 2254 cm^{-1}. ^{g} ν_{max}(CN) 2252 cm^{-1}.

Table 2. ^{1}H and ^{13}C NMR Data^a

compd	^{1}H/δ	^{13}C/δ^b
3^c	8.66 (d, 4H, NC_5H_4Me, J = 6), 7.29 (d, 2H, $C_6H_4NMe_2$, J = 9), 7.11 (d, 4H, NC_5H_4Me, J = 6), 6.54 (d, 2H, $C_6H_4NMe_2$, J = 9), 3.00 (s, 6H, $C_6H_4NMe_2$), 2.35 (s, 6H, NC_5H_4Me)	277.0^d (W≡C), 221.4^d (CO), 167.7 (CF_3CO_2), 151.3, 149.4, 124.8 (NC_5H_4Me), 150.4, 132.6, 128.9, 126.0 ($C_6H_4NMe_2$) 111.2 (CF_3CO_2), 40.3 ($C_6H_4NMe_2$), 21.3 (NC_5H_4Me)
4a^e	9.26 (d, 2H, $N_2C_{10}H_8$, J = 5), 8.15 (d, 2H, $N_2C_{10}H_8$, J = 8), 8.08 (t, 2H, $N_2C_{10}H_8$, J = 8), 7.51 (t, 2H, $N_2C_{10}H_8$, J = 7), 7.05 (d, 2H, $C_6H_4NMe_2$, J = 9), 6.36 (d, 2H, $C_6H_4NMe_2$, J = 9), 2.84 (s, 6H, $C_6H_4NMe_2$)	281.3^d (W≡C), 225.0^d (CO), 162.3 (CF_3CO_2), 156.9, 150.9, 140.8, 123.9, 119.5 ($N_2C_{10}H_8$) 155.5, 134.2, 131.8, 127.5 ($C_6H_4NMe_2$), 111.5 (CF_3CO_2) 40.3 ($C_6H_4NMe_2$)
4b^f	7.17 (d, 2H, $C_6H_4NMe_2$, J = 9), 6.54 (d, 2H, $C_6H_4NMe_2$, J = 9), 3.16 (s, 6H, CH_2NMe), 2.95 (s, 6H, $C_6H_4NMe_2$), 2.87 (s, 6H, CH_2NMe), 2.86−2.80 (m br, 4H, CH_2NMe)	279.1^d (W≡C), 222.5^d (CO), 168.8 (CF_3CO_2), 151.9, 139.6, 131.2, 114.4 ($C_6H_4NMe_2$), 111.5 (CF_3CO_2), 61.5, 58.4, 52.2 (CH_2NMe), 40.5 ($C_6H_4NMe_2$)
5a^e	9.35 (d, 2H, $N_2C_{10}H_8$, J = 5), 8.78 (d, 2H, $N_2C_{10}H_8$, J = 8), 8.22 (t, 2H, $N_2C_{10}H_8$, J = 8), 7.66 (t, 2H, $N_2C_{10}H_8$, J = 7), 7.05 (d, 2H, $C_6H_4NMe_2$, J = 9), 6.46 (d, 2H, $C_6H_4NMe_2$, J = 9), 2.91 (s, 6H, $C_6H_4NMe_2$), 2.11 (s, 3H, MeCN)	282.1^d (W≡C), 224.9^d (CO), 156.9, 151.7, 140.3, 129.4, 118.6 ($N_2C_{10}H_8$), 155.5, 131.8, 130.9, 127.6 ($C_6H_4NMe_2$), 114.3 (MeCN), 40.2 ($C_6H_4NMe_2$), 1.5 (MeCN)
5b^f	7.19 (d, 2H, $C_6H_4NMe_2$, J = 9), 6.54 (d, 2H, $C_6H_4NMe_2$, J = 9), 3.21 (s, 6H, CH_2NMe), 2.97 (s, 6H, $C_6H_4NMe_2$), 2.94 (s, 6H, CH_2NMe), 2.87−2.78 (m br, 4H, CH_2NMe), 2.30 (s, 3H, MeCN)	279.5^d (W≡C), 221.6^d (CO), 147.4, 142.1, 131.1, 118.7 ($C_6H_4NMe_2$), 113.2 (MeCN), 61.2, 58.3, 52.3 (CH_2NMe), 40.5 ($C_6H_4NMe_2$), 1.4 (MeCN)

^{a} Chemical shifts (δ) in ppm, coupling constants (J) in Hz, measurements at 298 K. ^{b} ^{1}H-decoupled, chemical shifts are positive to high frequency of $SiMe_4$. ^{c} Measured in CD_2Cl_2. ^{d} ^{183}W satellite peaks too weak to be observed, even at −50 °C. ^{e} Measured in d_8-THF. ^{f} Measured in $CDCl_3$.

lent carbonyl carbons at δ 222.5 in the ^{13}C{^{1}H} NMR spectrum. In the same spectrum, the alkylidyne NMe_2 group has a resonance at δ 40.5. The invariance of these data from complexes **3** through **4b** would seem to suggest similar electron density distributions along the metal-alkylidyne-aryl-donor group assembly. Finally, the cationic acetonitrile adduct, [W(≡$CC_6H_4NMe_2$-4)(NCMe)$(CO)_2${κ^2-$Me_2N(CH_2)_2NMe_2$}][PF_6] (**5b**), analogous to the complex salt **5a**, has been synthesized in a similar manner, by treatment of complex **4b** with $TlPF_6$ in MeCN/THF. Once again, the ν_{max}(CN) absorption arising from the complex is observed at 2252 cm^{-1} and ν_{max}(CO) resonances appear at 1984 and 1892 cm^{-1}, shifted to higher energy as expected with the formation of a cationic adduct from its neutral parent complex **4b**. There also appears to be little impact on the characteristic NMR resonances for compound **5b** versus those of complex **4b**, with the exception of the appearance of signals at δ 2.30 and 1.4 in the ^{1}H and ^{13}C{^{1}H} NMR, respectively, for the MeCN methyl group and at δ 113.2 for the nitrilo carbon in the latter spectrum. The alkylidyne aryl system is invariant with respect to the parent complex **4b**, with the alkylidyne W≡C carbon resonating at δ 279.5 and the equivalent carbonyl carbons at δ 221.6 in the ^{13}C{^{1}H} NMR spectrum. The remaining resonances in both the ^{1}H and ^{13}C{^{1}H} NMR spectra are also very similar to those of complex **4b**. In terms of the level of electron density, it thus seems that acquisition of the cationic charge at the metal center is offset by the substitution with a somewhat stronger donor MeCN ligand, despite the latter's improved π-acidity over the $CF_3CO_2^-$ ligand. Indeed, the very slight increase in ν_{max}(CO) values (ca. 10 cm^{-1}) observed upon formation of **4**,**5b** from **4**,**5a** bears this out, in addition to the above-discussed NMR characteristics.

Photoluminescence. In contrast to the previously mentioned complexes **2b** and **2c**, solutions of all five complexes **3**−**5b** are emissive in the visible region in CH_2Cl_2 at ambient temperatures upon UV photoexcitation. Photoabsorption and -emission data for the five complexes are presented in Table 3. Representative excitation/emission spectra are given in Figure 1 for complex **4a**. Structureless blue emission (ca. 450 nm) is common to all five complexes, with excitation and emission wavelengths being all but invariant. The presence of the 2,2′-dipyridyl ligand clearly enhances this emission with significant quantum yields for complexes **4a** ($\Phi_{451} = 1.04 \times 10^{-2}$) and **5a** ($\Phi_{450} = 1.26 \times 10^{-2}$) versus $\Phi_{448} = 1.25 \times 10^{-3}$ for complex **3**. This would seem to indicate that the emissive absorption is primarily confined to the W≡$CC_6H_4NMe_2$-4 $\pi-\pi^*$ system, with the presence of the 2,2′-dipyridyl ligand stimulating radiative emission without directly impacting the electronic transitions.

The electronic absorption spectrum of complex **4a** (Figure 2) indicates that a shoulder at ca. 315 nm

Table 3. UV−Vis Absorption and Photoluminescence Data[a]

compd	λ_{max}/nm ($\epsilon \times 10^{-3}$/M^{-1} cm^{-1})	λ_{ex}, λ_{em}/nm[b]	$\Phi_{em} \times 10^3$ [c]
3	290 (14.50), 372 (18.07), 468 (2.93)	317, 448 472, 540	1.25 0.970
4a	300 (18.60), 315 (sh), 371 (18.60), 470 (3.34)	317, 451 470, 580	10.4[d] 6.37[e]
4b	286 (12.10), 364 (17.00), 449 (1.70)	317, 453 458, 554	2.03 0.700
5a	249 (17.50), 308 (16.90), 380 (9.00), 472 (6.50)	317, 450	12.6
5b	289 (11.90), 363 (19.70), 449 (1.65)	316, 451 410, 536	2.14 0.121

[a] Measured in CH_2Cl_2 (25 μM) at 298 K. [b] λ_{ex} = excitation maximum, λ_{em} = emission maximum. All spectra are excitation and emission corrected. [c] Emission quantum yield, Φ_{em}, relative to 9-cyanoanthracene (Φ_{em} = 1.00), ±10%, corrected for self-absorption. [d] Lifetime, τ_{451} = 4.4 ns. [e] Lifetime, τ_{580} = 1.1 ns (82%) and 5.3 ns (18%).

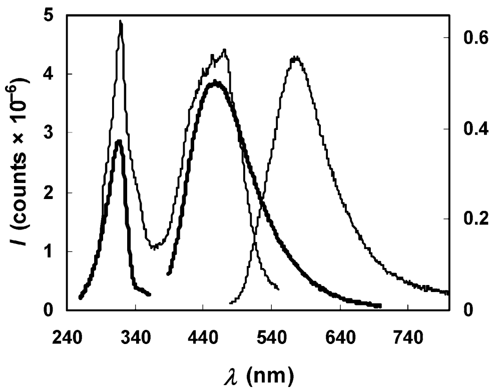

Figure 1. Photoexcitation and -emission spectra for a 25 μM solution of complex **4a** in CH_2Cl_2: (**—**) λ_{ex} = 317, λ_{em} = 451 nm (left ordinate); (—) λ_{ex} = 470, λ_{em} = 580 nm (right ordinate).

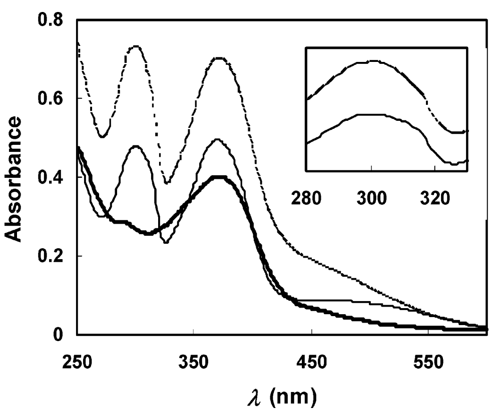

Figure 2. Electronic absorption spectra for 250 μM solutions of complexes **3** and **4a**: (**—**) **3** in CH_2Cl_2; (—) **4a** in CH_2Cl_2; (- - -) **4a** in MeCN. Inset shows expansion of absorbances for **4a** in CH_2Cl_2 and MeCN between 280 and 330 nm.

appears to be the emissive absorption, which is very slightly blue-shifted in MeCN solution, indicating little change in polarity upon absorption, typical for significant metal−ligand mixing in the ground state. A close match between the absorption shoulder and the excitation peak is noteworthy (Figure 3). Unfortunately this absorption is obscured by the stronger, higher energy absorption in the UV−vis spectra of the other complexes **4b**, **5a**, and **5b**. Although the 4-methylpyridine complex

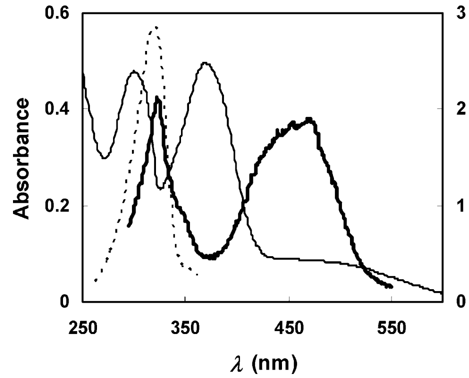

Figure 3. Electronic absorption spectrum (—) for a 250 μM solution of complex **4a** and photoexcitation spectra for a 2 μM solution of the same complex at λ_{em} = 451 nm (- - -) and λ_{em} = 580 nm (**—**) at ca. 4 × slit width.

3 absorbs in this vicinity, it is much weaker than for complex **4a**. Further analysis shows that absorption at ca. 370 nm is common to both complexes **3** and **4a**, is not solvatochromic, and is nonemissive. This might be suggestive of a "pure" $\pi_{W\equiv CAr}-\pi^*_{W\equiv CAr}$ transition, while that at ca. 315 nm, which is responsible for radiative emission, is "contaminated" by possible LMCT character, namely, $n_{NMe_2}-\pi^*_{W\equiv CAr}$. This absorption would not necessarily be classed as a charge transfer band, thanks to significant lone-pair-ligand−metal mixing in the ground state, which is in turn due to the expected planarity and parallel orientation of the NMe_2 group with respect to the aryl−alkylidyne π framework. Supporting this notion is the absence of emission for the complex **2c**, which possesses no such donor group on the alkylidyne moiety. Our own measurements on CH_2Cl_2 solutions of the *para*-toluidyne complex [$W(\equiv CC_6H_4$-Me-4)$(O_2CCF_3)(CO)_2(NC_5H_4Me\text{-}4)_2$] also show a complete absence of blue fluorescence.

The band-shape asymmetry between excitation and emission spectra noted in Figure 1, common to measurements of this higher energy emission in all the complexes, is symptomatic of some nuclear rearrangement. Furthermore, these features are independent of the presence of triplet sensitizers (e.g., O_2), implying that a distorted singlet excited state with substantial metal d character is responsible for this blue emission. Measurements in MeTHF (2-methyltetrahydrofuran) at 77 K revealed a more structured emission, although essentially wavelength invariant (λ_{em} = 450 nm) with a vibronic progression, $\Delta\bar{\nu}_{0,1} \approx$ 1350 cm^{-1} (Figure 4). This closely matches a strong vibration at 1370 cm^{-1} in the IR spectrum (Supporting Information), which can be assigned to the aromatic-C−N stretch for the NMe_2 group and is just outside the expected range (1310−1360 cm^{-1}) for such a vibrational excitation in an organic tertiary aromatic amine.[13] The excitation peak (λ_{ex} = 290 nm) was slightly blue-shifted by some 2940 cm^{-1} and comparatively broader with some structure as well.

Lifetime measurements of CH_2Cl_2 solutions at 298 K and MeTHF solutions at 77 K using a pulsed N_2 laser (λ = 337 nm) indicate $\tau_{450} \leq$ 10 ns for all the new complexes, further supporting exclusive singlet spin

(13) Mohan, J. *Organic Spectroscopy−Principles and Applications*; CRC Press: New York, 2000; pp 60−61.

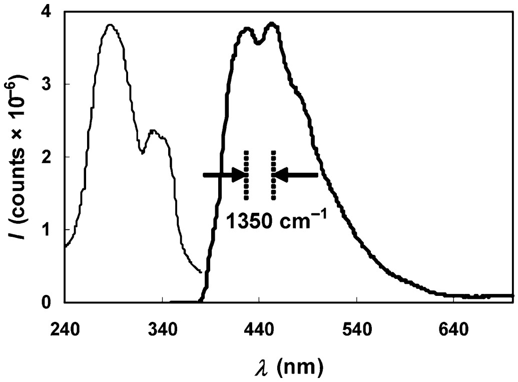

Figure 4. Photoexcitation and -emission spectra for a 25 μM solution of complex **4a** in MeTHF at 77 K: (–) λ_{ex} = 290 nm; (**—**) λ_{em} = 450 nm.

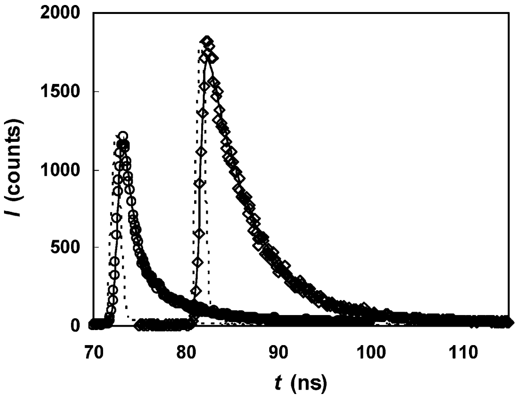

Figure 5. Fluorescence decay curves for λ_{em} = 451 nm (◇, τ = 4.4 ns) and 580 nm (○, τ = 1.1 ns (82%), 5.3 ns (18%)) with their respective fits (–). Instrument response measurements are indicated (- - -).

character in the excited state. Closer analysis of complex **4a** at ambient temperatures using a faster pulsed N_2 laser revealed a single-exponential decay with τ_{451} = 4.4 ns (Figure 5). Such short lifetimes coupled with high quantum yields for high-energy visible light emission, although expected from the Einstein *A* coefficient,[14] are highly unusual for organometallic complexes given the alternate photoreactive pathways usually available following UV excitation.

However, these observations permit us to pinpoint the nature of the distortion. It has been reported by Lin and co-workers that twisted intramolecular charge transfer (^{1}TICT) rotamer formation in the molecule 4-$Me_2NC_6H_4$-$(CH{=}CH)_3C_6H_4NO_2$-4 is responsible for very short-lived fluorescence at λ_{em} = 525 nm in hexane.[15] Similar photophysical properties were concomitantly reported by Whitten and co-workers for the related species 4-Me_2-$NC_6H_4(CH{=}CH)_nC_6H_4NO_2$-4 ($n$ = 1−3),[16] and the phenomenon has been extensively studied by Rettig[17] following its discovery by Grabowski, Siemiarczuk, and co-workers.[18] Although Lin's emission was weak to moderate, even at 77 K, it was reported to have no

Scheme 1. Implication of an Emissive Twisted Intramolecular Charge Transfer (TICT) Complex in the Blue Fluorescence of the Complexes 3−5[a]

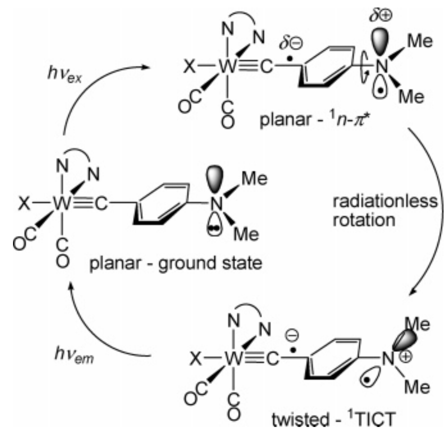

[a] X^- = $CF_3CO_2^-$, MeCN; N⁀N = 2 × NC_5H_4Me-4, κ^2-2,2′-$(NC_5H_4)_2$, κ^2-$Me_2N(CH_2)_2NMe_2$. The symbols $\delta\oplus/\delta\ominus$ do not represent overall charge distribution, but partial charge dislocation resulting from the transition. Once twisted, full $\oplus/\ominus$ charge separation must occur.

detectable long lifetime (which we take to imply as a sub-10 ns time scale from the experimental parameters given), as opposed to a coexisting nontwisted excited state (planar intramolecular charge transfer, PICT), which showed fluorescence at λ_{em} = 439 nm ($5 \le \tau \le 25$ ns) and an associated long-lived (τ = 700 ms) $\pi-\pi^*$ emission at λ_{em} = 453 nm at 77 K. The mechanism of the distortion involved a simple 90° twisting of the NMe_2 group relative to the planar hyperconjugated architecture of the diphenylhexatriene backbone. These photophysical experimental results have been supported by a range of high-level computational calculations, including time-dependent density functional theory studies, on organic aromatic acceptor−donor chromophores, 4-$ZC_6H_4NR_2$ (Z = acceptor group, e.g., CN, NO_2, R = Me).[19] We propose a similar ^{1}TICT state for the complexes **3**−**5** (Scheme 1), which is consistent with that of the organic analogue 4-$Me_2NC_6H_4(CH{=}CH)_3C_6H_4$ NO_2-4, although the organometallic tungsten complexes clearly emit very strongly in solution at ambient temperatures. A nondistorted triplet excited state is precluded, as one would expect such a metal-purturbed system to have a much longer decay lifetime. Indeed the long-lived undistorted phosphorescent state observed in Lin's organic system is absent in the tungsten alkylidynes, possibly due to efficient singlet−singlet crossover to a second metal-based rapidly relaxing fluorescent state (vide infra). It is also noteworthy that Rettig attributes sulfur d orbital participation in the TICT emission from 4,4′-dimethylaminophenyl sulfone to a diminished nonradiative singlet-to-triplet transition.[20]

It was also reported for 4-$Me_2NC_6H_4(CH{=}CH)_3C_6H_4$-$NO_2$-4 that, along with expected red-shifting of λ_{em}, a decrease in ^{1}TICT emission was observed as solvent polarity increased and accredited to strong intermolecular bonding, particularly in hydrogen-bonding sol-

(14) Hollas, J. M. *Modern Spectroscopy*, 3rd ed.; Wiley: New York, 1996; p 27.
(15) Lin, C. T.; Guan, H. W.; McCoy, R. K.; Spangler, C. W. *J. Phys. Chem.* **1989**, *93*, 39.
(16) Shin, D. M.; Whitten, D. G. *J. Phys. Chem.* **1988**, *92*, 2945.
(17) Rettig, W. *Angew. Chem., Int. Ed. Engl.* **1986**, *25*, 971, and references therein.
(18) Grabowski, Z.; Rotkiewicz, K.; Siemiarczuk, A.; Cowley, D. J.; Baumann, W. *Nouv. J. Chim.* **1979**, *3*, 443.
(19) (a) Jamorski Jödicke, C.; Lüthi, H. P. *J. Am. Chem. Soc.* **2003**, *125*, 252. (b) Jamorski Jödicke, C.; Lüthi, H. P. *J. Chem. Phys.* **2002**, *117*, 4146. (c) Jamorski Jödicke, C.; Lüthi, H. P. *J. Chem. Phys.* **2002**, *117*, 4157.
(20) Rettig, W.; Chandross, E. A. *J. Am. Chem. Soc.* **1985**, *107*, 5617.

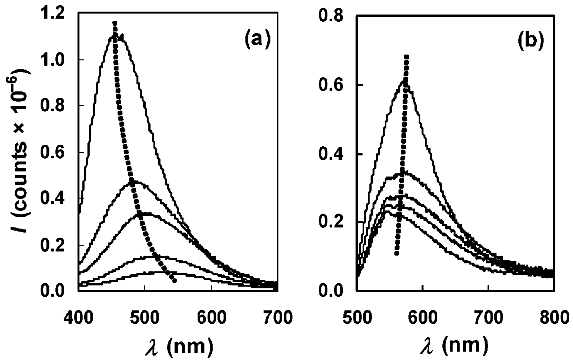

Figure 6. Photoexcitation and -emission spectra for 2 μM solutions of complex **4a** in CH_2Cl_2/MeCN mixtures in order of decreasing intensity: 100:0 (neat CH_2Cl_2); 80:20; 50:50; 20:80; 0:100 (neat MeCN): (a) higher energy ^{1}TICT emission; (b) lower energy $^1d_W-\pi^*_{W\equiv CAr}$ emission.

vents. This made emissive relaxation back to a planar ground state less likely, and the ratio of the intensities of TICT/PICT emission thus decreased in the more polar solvents. We too observe a dramatic reduction in emission intensity in MeCN (ca. 90%) versus that observed in CH_2Cl_2 solutions, especially for complex **4a**, which also demonstrates substantial red-shifting of the emission maximum from $\lambda_{em} = 450$ nm in CH_2Cl_2 to 535 nm in MeCN (Figure 6a) for this complex, while λ_{ex} remains virtually unchanged. Static singlet quenching by MeCN should not account for this, and intermolecular solvent−solute interference with the ground state configuration, as has been observed with 4-$Me_2NC_6H_4(CH{=}CH)_3C_6H_4$-$NO_2$-4, is a more likely explanation.[15] An even steeper decline (ca. 85%) in emission intensity was noted for the same molarity of complex **4a** in a solution of CH_2Cl_2/EtOH (50:50).

Complexes **3** and **4a** show a second broader structureless emission, both with similar excitation ($\lambda_{ex} \approx 470$ nm) and with complex **3** emitting at $\lambda_{em} = 580$ and complex **4a** significantly blue shifted at $\lambda_{em} = 540$ nm. While the quantum yield for this emission in complex **3** ($\Phi_{540} = 9.70 \times 10^{-4}$) is modest, that in complex **4a** ($\Phi_{580} = 6.37 \times 10^{-3}$) is again noticeably enhanced by the presence of the 2,2′-dipyridyl ligand. Curiously, however, radiative emission in this second wavelength regime is absent for cationic derivative complex **5a**. Here it seems that the intramolecular quenching by the 2,2′-dipyridyl ligand, identified by Mayr in complex **1c**, might now be operating, especially in light of the optical behavior of compound **5b**, discussed below. This may be due to a closer energy match between the 2,2′-dipyridyl and $W{\equiv}CC_6H_4NMe_2$-4 π^* orbitals. Band-shape similarity between excitation and emission spectra, both at 298 K in CH_2Cl_2 (Figure 1) and at 77 K in MeTHF, suggests that these are the same parity-forbidden, spin-allowed $d_W-\pi^*_{W\equiv CAr}$ singlet−singlet transitions identified in complexes **1**.[8] Furthermore, the moderately low molar absorbivity at these excitation wavelengths in the electronic absorption spectra of the complex (Table 3, Figure 2) supports the notion of substantial d character in the $\pi^*_{W\equiv CAr}$ state, this feature also being identified in the complexes **1**. An excellent match between the broad absorption peak and photoexcitation spectrum is apparent (Figure 3). A distinct lack of rigidochromism of the emission wavelength in the photoemission spectra measured in MeTHF at 77 K is also supportive of this assignment. Closer analysis of the photoexcitation spectrum measured back to 290 nm very informatively revealed a further excitation peak at $\lambda_{ex} = 319$ nm, again overlapping with the absorption that also produces the higher energy ^{1}TICT emission (Figure 3). This same excitation peak was still readily apparent at emission wavelengths beyond 650 nm, where emission from the ^{1}TICT state has fallen close to zero. However, the narrower Stokes shift (4035 cm^{-1} (**4a**) and range 2700−5700 cm^{-1} for all compounds) observed for the photoluminescence in our complexes, resulting in generally yellow light emission rather than the lower energy red light produced by the complexes **1**, is highly suggestive of strong $^1d_W-\pi^*_{W\equiv CAr}$ singlet character as opposed to emission from a triplet manifold. Insensitivity of the photoluminescence of complexes **3** and **4a** to the presence of triplet sensitizers (O_2, 10 mM anthracene) once again supports this. Furthermore, time-resolved fluorescence using a fast pulsed N_2 laser again yielded a very short lifetime, which was biexponential with $\tau_{580} = 1.1$ ns (82%) and 5.3 ns (18%) at $\lambda_{em} = 580$ nm (Figure 5). Both these values, which may result from closely energy-matched but not identical $^1d_W-\pi^*_{W\equiv CAr}$ states resulting from the low symmetry of the complex, are considerably shorter than the accepted range for phosphorescence from a $^3d_W-\pi^*_{W\equiv CAr}$ state (10−500 ns) in solution at ambient temperatures.[7] As with the higher energy emission of complex **4a**, a significant decrease in intensity of emission is noted in MeCN, although there are two important differences: (i) the intensity decreases by only ca. 65% from neat CH_2Cl_2 to neat MeCN, and (ii) there is a very slight blue shifting in emission wavelength from $\lambda_{em} = 580$ to 565 nm (Figure 6b). Although it is very tempting to conclude a singlet state is indeed responsible for this emission, a very short-lived phosphorescent $^3d_W-\pi^*_{W\equiv CAr}$ state might account for the lack of intersystem crossing between the two emissive states. On the other hand, this is exceedingly unlikely with $\tau_{580} = 1.1$ ns, and the absence of a singlet−singlet interaction in this case can be accounted for, if one of the excited fluorescent states is a very short-lived distorted species, while the other is an undistorted metal-based singlet state with a comparable or shorter lifetime, as has been found. Even a triplet assignment to the $\tau_{580} = 5.3$ ns component would be tenuous at best. Such short-lived phosphorescence would be very difficult if not impossible to detect through energy transfer experiments and as such cannot be ruled out.

Absence of the so-called "normal" fluorescence (at even shorter wavelength) from a nondistorted $^1n_{NMe_2}-\pi^*_{W\equiv CAr}$ state normally accompanying ^{1}TICT emission may be attributed to the efficient distribution of energy to the lower energy $^1d_W-\pi^*_{W\equiv CAr}$ state through intersystem crossover (IS, Scheme 2) as well as to the ^{1}TICT state itself. Communication between the two nondistorted singlet states of complex **4a** is strongly supported by the observation of two photoexcitation peaks at 319 and 470 nm (Figures 1 and 3) corresponding to the yellow emission.

The TMEDA complexes **4b** and **5b** both show the dual emission characteristics of complexes **3** and **4a** (λ_{em} = 453, 554 nm (**4b**) and 451, 536 nm (**5b**), Table 3), although it should be noted that while the lower energy

Scheme 2. Generalized Relative Energy Diagram for Dual Fluorescence from Complex 4a (not drawn to scale)[a]

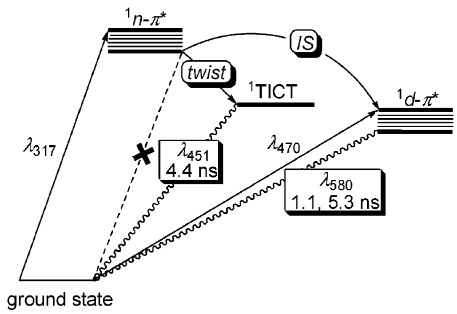

[a] It is assumed that both radiative emissions are accompanied by nonradiative relaxation.

yellow emission of **5a** is completely quenched, that in **5b** is detectable, though more than an order of magnitude weaker than observed for the strongest emission by **4a** at λ_{em} = 580 nm. These observations verify that the orthogonal 2,2′-dipyridyl ligand is itself not so intimately involved in the emission processes, at least in terms of orbital contribution; that is, luminescence characteristics are confined mainly to the $W{\equiv}CC_6H_4$-NMe_2-4 backbone and again serve to emphasize the fact that, with the exception of the second, lower energy emission of complex **5a** (or rather lack thereof), the 2,2′-dipyridyl ligand not only does not quench emission but actually enhances it. The reason for this enhancement is most likely due to the increased stereochemical rigidity afforded by the 2,2′-dipyridyl chelating moiety. Compounds **3**, **4b**, and **5b**, with their more flexible bis(4-methylpyridine) and TMEDA ligands, possess increased internal rotational degrees of freedom, which may serve to increase the efficiency of nonradiative decay relative to compounds **4a** and **5a**.

At this time, further work is in process to elucidate the precise impact of polypyridyl ligands on the nature of the photoluminescence in tungsten alkylidyne complexes, by synthesizing complexes with modified 2,2′-dipyridyl rings. Further work is also under way to extend the hyperconjugated tungsten−alkylidyne backbone, using Sonogoshira coupling processes, which have been successfully investigated by Mayr and co-workers,[21] to couple the W≡C unit with acetylenic dimethylanilino molecules, for example. Such variations may lead to a more comprehensive tuning of the fluorescent output. Most importantly, increased stereochemical rigidity of the bidentate and potentially tridentate ligands will be targeted in an attempt to increase the efficiencies of emission, especially the blue TICT photoluminescence.

Conclusions. We have isolated several tungsten alkylidyne complexes using established synthetic techniques and workup procedures, yielding highly pure materials for photophysical analysis. With the exception of one compound, **5a**, which displays a single blue fluorescence band, all the complexes display strong dual blue-yellow fluorescence, with almost no variation of the higher energy blue emission wavelength (λ_{em} = 450 nm) from one complex to the other. The mechanisms involve short-lived singlet manifolds resulting from distinct ^{1}TICT n_{NMe_2}−$\pi^*_{W\equiv CAr}$ and ^1d_W−$\pi^*_{W\equiv CAr}$ transitions. The latter has been previously reported for group 6 metal alkylidynes, but as a lower energy triplet emission only. There is to our knowledge no precedence for either singlet fluorescence in group 6 metal alkylidyne complexes nor TICT emission in organometallic complexes in general, let alone with the intensity and efficiency described above. The anomalously high quantum yields for complexes **4a** and **5a**, in particular, may be attributed to short lifetimes for both emissions, as well as the impact of the stereorigid 2,2′-dipyridyl ligand. Other current work is revealing interesting electrochemical behavior for these complexes in solution, especially the cationic complex **5a**, which displays electrodeposition characteristics upon reduction. These results will be reported in due course.

Experimental Section

All synthetic procedures were conducted under an atmosphere of dry nitrogen or argon using Schlenk-line and glovebox techniques. Solvents were freshly distilled under argon from appropriate drying agents before use. Celite pads used for filtration were 3 × 5 cm, and alumina (Brockmann III) columns were 2 × 10 cm. Tungsten hexacarbonyl and thallium(I) hexafluorophosphate were used as purchased from Strem Chemicals. The reagents 4-bromo-*N*,*N*-dimethylaniline, trifluoroacetic anhydride, 4-methylpyridine, 2,2′-dipyridyl, and *N*,*N*,*N*′,*N*′-tetramethylethylenediamine were used as purchased from Aldrich. The molarities of solutions of *n*-butyllithium (1.6 M in hexane), purchased from Aldrich, were checked by titration prior to use.

Spectroscopic Measurements. All solution measurements were made at 298 K. IR measurements were made using solution cells in a Perkin-Elmer RX-I FT-IR spectrometer. UV−vis measurements were made between 220 and 800 nm with a Shimadzu 2530 UV−visible absorption spectrophotometer. NMR measurements were recorded using a Varian Gemini 300 MHz spectrometer: ^{1}H (300.0 MHz) and ^{13}C (75.4 MHz).

Fluorometry Measurements. Photoluminescence measurements were made with a PTI QM4 fluorescence spectrophotometer with a Xe arc lamp light source and digital PMT detector. Emission and reference source gain excitation corrections were applied to all steady state data. Slit widths were set at 2−5 nm. Appropriate cutoff filters were used to eliminate peaks due to solvent Raman-shifted bands and excitation harmonics. Solution samples (2−25 μM) at ambient temperatures were measured in a quartz sample cuvette with Schlenk attachment to deoxygenate samples. Samples measured at 77 K were degassed and analyzed in a quartz NMR tube with Schlenk attachment and set in a quartz-bottomed Dewar flask in an argon-filled sample chamber.

Quantum yields were assessed by comparison of integrated peak intensities between those of the complexes at each of their emission wavelengths and the singlet emission from deoxygenated 9-cyanoanthracene in hexane, which has Φ_{em} = 1.00. Concentrations of the complex solutions were adjusted to give accurately measured absorbances of ca. 0.1 A at λ_{ex}. A standard solution of 9-cyanoanthracene was similarly created (λ_{ex} = 399 nm), and its integrated emission intensity measured using an optical density (OD1) filter at the emission monochromator entrance at consistently fixed slit widths for all measurements. Quantum yields were then calculated according to

$$\Phi_{em} = \frac{I_{int,x}/f_x}{(I_{int,c}/f_c) \times 100}$$

(21) Yu, M. P. Y.; Cheung, K.-K.; Mayr, A. *J. Chem. Soc., Dalton Trans.* **1998**, 2373.

where I_{int} = integrated intensity and f = fraction of light absorbed for solutions of the complexes (x) and of 9-cyanoanthracene (c). Emission quantum yields, I_{int}, were corrected for self-absorption using transmission data parameters from the UV−vis absorption spectra over the width of the emission band.

For all compounds the fluorescence decays were measured using a digital storage oscilloscope-based instrument.[22] Excitation was provided by a small N_2 laser operating at 20 Hz using no dye (λ_{ex} = 337 nm) or 4 × 10^{-3} M coumarin-440 in EtOH (λ_{ex} = 440 nm). A small fraction of the excitation beam was reflected onto a Texas Optoelectronics TIED 56 photodiode, which triggered the oscilloscope.[23] Emission from the sample was detected with a fast-wired Burle 931-A photomultiplier tube[24] after passing through a small monochromator with 2.2 nm resolution. Emission was monitored at 451 and 580 nm in consecutive experiments. The PMT output was sent into a Tektronix TDS-350 digital storage oscilloscope. For each laser pulse the oscilloscope collected a complete fluorescence decay. Results from 256 laser pulses were averaged for each fluorescence decay. At least five decays were averaged to produce each lifetime. Accurate fluorescence decays from compound **4a** were measured with a PTI model TM-3/2005 lifetime fluorescence spectrophotometer. The instrument employed a PTI GL-330 pulsed nitrogen laser pumping a PTI GL-302 tunable dye laser as an excitation source and a proprietary stroboscopic detection system with an R928 photomultiplier. The decays were analyzed with a PTI FeliX32 advanced analysis package utilizing a discrete multiexponential fitting function and iterative reconvolution. An attempt was made to check for any long-lived emission within the 600−700 nm range utilizing the nitrogen/dye laser combo and a gated phosphorescence detector with an R928 photomultiplier. No emission with a lifetime longer than 500 ns (gated detector resolution limit) was observed.

Synthesis of [W(≡CC$_6$H$_4$NMe$_2$-4)(O$_2$CCF$_3$)(CO)$_2$(NC$_5$H$_4$Me-4)$_2$], 3. The procedure follows the general method of Mayr.[9,10] The compound 4-bromo-*N*,*N*-dimethylaniline (2.84 g, 14.2 mmol) was dissolved in Et$_2$O (30 mL). To this solution was added dropwise LiBu^n (8.88 mL, 1.6 M in hexane, 14.2 mmol), and the resulting reaction mixture was stirred for 1 h at room temperature. After this time, [W(CO)$_6$] (5.00 g, 14.2 mmol) was suspended in Et$_2$O (50 mL). The cloudy yellow solution of Li[C$_6$H$_4$NMe$_2$-4] was added slowly via cannula transfer to the [W(CO)$_6$] suspension in aliquots of ca. 1.5 mL, producing the characteristic brilliant red-orange solution of the anionic tungsten acyl complex [W(CO)$_5${C(O)-C$_6$H$_4$NMe$_2$-4}]$^-$. The solution was stirred for 2 h, and then the solvent was removed in vacuo. The resulting orange-brown residue was redissolved in CH$_2$Cl$_2$ (30 mL) and filtered through Celite. The filtrate was then cooled to −78 °C, and trifluroacetic anhydride (2.00 mL, 14.2 mmol) was added to the solution dropwise, forming a deep violet solution with the evolution of CO gas. The solution was allowed to warm to −35 °C, and then 4-methylpyridine (5.53 mL, 56.8 mmol) was added to the solution dropwise, affording a change in color from violet to green with further evolution of CO. The reaction mixture was then allowed to warm to room temperature and stirred for 48 h. After this time the solvent was removed in vacuo and the solution was washed with hexanes (5 × 50 mL) to remove excess 4-methylpyridine. The residue was dissolved in the minimum volume of CH$_2$Cl$_2$−hexanes (20 mL, 4:1) and chromatographed using the same solvent mixture. A first yellow fraction containing 4-methylpyridine was eluted and discarded, then followed by an intense yellow band, which was collected. Removal of the solvent in vacuo and recrystallization from CH$_2$Cl$_2$−hexanes (20 mL, 1:1) at −78 °C, washing with hexanes (3 × 50 mL), and drying in vacuo afforded yellow microcrystals of [W(≡CC$_6$H$_4$NMe$_2$-4)(O$_2$CCF$_3$)(CO)$_2$(NC$_5$H$_4$Me-4)$_2$], **3** (3.19 g).

Synthesis of [W(≡CC$_6$H$_4$NMe$_2$-4)(O$_2$CCF$_3$)(CO)$_2${κ^2-2,2′-(NC$_5$H$_4$)$_2$}], 4a. Complex **3** (0.15 g, 0.22 mmol) and 2,2′-dipyridyl (0.04 g, 0.25 mmol) were dissolved in CH$_2$Cl$_2$ (25 mL), and the solution was stirred at room temperature for 24 h, resulting in a brilliant red solution. Solvent was removed in vacuo, and the residue was washed with hexanes (5 × 10 mL) and then recrystallized from CH$_2$Cl$_2$−hexanes (10 mL, 1:1), yielding red microcrystals of [W(≡CC$_6$H$_4$NMe$_2$-4)(O$_2$CCF$_3$)-(CO)$_2${κ^2-2,2′-(NC$_5$H$_4$)$_2$}], **4a** (0.15 g).

Synthesis of [W(≡CC$_6$H$_4$NMe$_2$-4)(O$_2$CCF$_3$)(CO)$_2${κ^2-Me$_2$N-(CH$_2$)$_2$NMe$_2$}], 4b. Using a similar procedure, complex **3** (0.15 g, 0.22 mmol) and *N*,*N*,*N*′,*N*′-tetramethylethylenediamine (38 μL, 0.25 mmol) afforded yellow microcrystals of [W(≡CC$_6$H$_4$NMe$_2$-4)(O$_2$CCF$_3$)(CO)$_2${κ^2-Me$_2$N(CH$_2$)$_2$NMe$_2$}], **4b** (0.13 g).

Synthesis of [W(≡CC$_6$H$_4$NMe$_2$-4)(NCMe)(CO)$_2${κ^2-2,2′-(NC$_5$H$_4$)$_2$}][PF$_6$], 5a. Complex **4a** (0.10 g, 0.16 mmol) was combined with TlPF$_6$ (0.06 g, 0.17 mmol). A mixture of THF and MeCN (27 mL, 25:2) was then added and stirred for 48 h, producing a cloudy red solution. Solvent was removed in vacuo, and the residue was redissolved in CH$_2$Cl$_2$ and filtered through Celite. Following removal of solvent in vacuo and recrystallization from CH$_2$Cl$_2$−hexanes (10 mL, 1:1), red microcrystals of [W(≡CC$_6$H$_4$NMe$_2$-4)(NCMe)(CO)$_2${κ^2-2,2′-(NC$_5$H$_4$)$_2$}][PF$_6$], **5a** (0.11 g), were formed.

Synthesis of [W(≡CC$_6$H$_4$NMe$_2$-4)(NCMe)(CO)$_2${κ^2-Me$_2$N-(CH$_2$)$_2$NMe$_2$}][PF$_6$], 5b. Using a similar procedure, complex **4b** (0.11 g, 0.17 mmol) and TlPF$_6$ (0.06 g, 0.17 mmol) afforded yellow microcrystals of [W(≡CC$_6$H$_4$NMe$_2$-4)(NCMe)(CO)$_2${κ^2-Me$_2$N(CH$_2$)$_2$NMe$_2$}][PF$_6$], **5b** (0.11 g).

Acknowledgment. Financial support from the ACS Petroleum Research Fund (Type G grant) and from the Saint Louis University Beaumont Faculty Development Fund is acknowledged. We thank Dr. Steven Buckner (SLU) for helpful advice.

Supporting Information Available: Full IR spectrum of complex **4a** measured in THF. This material is available free of charge via the Internet at http://pubs.acs.org.

OM0493006

(22) (a) Basile, F.; Cardamone, A.; Grinstead, K. D.; Miller, K. J.; Lytle, F. E.; Caprara, A.; Clark, C. D.; Heritier, J.-M. *Appl. Spectrosc.* **1993**, *47*, 207. (b) Buckner, S. W.; Forlines, R. A.; Gord, J. R. *Appl. Spectrosc.* **1999**, *53*, 115.

(23) Harris, J. M.; Barnes, W. T.; Gustafson, T. L.; Bushaw, T. H.; Lytle, F. E. *Rev. Sci. Instrum.* **1980**, *51*, 988.

(24) Harris, J. M.; Lytle, F. E.; McCain, T. C. *Anal. Chem.* **1976**, *48*, 2095.